Three Types Halogen Bond Interaction Studied Between Pyrazine And XF

Junyong Wu (nfjywu@163.com)
Taizhou University https://orcid.org/0000-0002-9706-9922

Hua Yan
Taizhou University

Hao Chen
Taizhou University

Yanxian Jin
Taizhou University

Aiguo Zhong
Taizhou University

Zhaoxu Wang
Hunan University of Science and Technology

Guoliang Dai
Suzhou University of Science and Technology

Research Article

Keywords: Parallel halogen bond, π-type halogen bond, SAPT, Conceptual DFT

Posted Date: October 22nd, 2021

DOI: https://doi.org/10.21203/rs.3.rs-970523/v1

Abstract

Except σ-type and π-type halogen bond, a new type of the parallel halogen bond interactions between pyrazine ($C_4H_4N_2$) and XF (X=F,Cl,Br and I) have been discovered at the MP2/aug-cc-pVTZ level. Through comparing the calculated interaction energy,we can know that the π-type halogen bonding interactions are weaker than the corresponding σ-type halogen bonding interactions, and parallel halogen-bond interactions are weaker than the corresponding π-type halogen bonding interactions in $C_4H_4N_2$-XF complexes. SAPT analysis shows that the electrostatic energy are the major source of the attraction for the σ-type halogen bonding interactions while the parallel halogen-bond interactions are mainly dispersion energy. For the π-type halogen bonding interactions in $C_4H_4N_2$-XF(X=F and Cl) complexes, electrostatic energy are the major source of the attraction, while in $C_4H_4N_2$-XF(X=Br and I) complexes the electrostatic term, induction and dispersion play equally important role in the total attractive interaction.NBO analysis, AIM theory and Conceptual DFT are also be utilized.

1. Introduction

In rencent years, the research of halogen bond has become a hot pot [1–16]. Electrostatic surface potentials is very versatile and powerful tool for discovering the interaction properties of halogen bonds [17–20]. Figure 1 illustrates that the electrostatic surface potentials of pyrazine ($C_4H_4N_2$) and dihalogen molecule XF (X=F, Cl, Br and I). Pyrazine has two nitrogen atoms on the 1,4-position to replace the carbon atom on the benzene ring. Compared with benzene analogues, pyrazine has many functions and reactivity. As can been see from Figure1 that a blueness region of nitrogen atom represents the most negative electrostatic surface potential, and there are positive electrostatic potentialsis on both the upper and lower surfaces of pyrazine ring. For the dihalogen molecule XF (X=F, Cl, Br and I), a red region with σ-hole was discovered on the tip of the X atom is the electropositive potential region. If the dihalogen molecule XF interacts with pyrazine,except σ-type and π-type halogen bond, a new type of the parallel halogen bond interactions between XF (X=F,Cl,Br,I) and pyrazine have been discovered.

In the present study, we discussed the three types halogen bond interaction between pyrazine and XF (X=F,Cl,Br and I). The purpose of this work is to explore the bonding nature of the σ-type halogen bond,π-type halogen bond and parallel halogen bonds of the studied dimer. The strength of the σ-type□π-type halogen bond and parallel halogen bond are also compared .

2. Methodology

The geometric structure of the dimers and isolated monomers were fully optimized by MP2 method with the aug-cc-pVTZ (aug-cc-pVTZ-pp for Br and I) basis sets [21, 22] applying the Gaussian 03 [23]. At the same time, the vibration frequency is calculated at the same lever to ensure that the optimized structure has real frequency and stability.The interaction energies have been corrected for basis bet superposition error (BSSE) using counterpoise method which is put forward by Boys and Bernardi [24].The single-point computations have been carried out on the MP2/aug-cc-pVTZ optimized geometry at CCSD(T)/aug-cc-

pVTZ level [25]. To understand the interaction of σ-type, π-type and parallel halogen bond of these dimeres, The NBO population analysis [26] was performed at the same level.

The electrostatic surface potentials on the 0.001 au were calculated by WFA-SAS procedure [27]. To further our understanding of the three types halogen bond interaction, the concept of DFT [28–30] is used to study the reaction properties of the interacting molecules in the σ-type,π-type and parallel halogen bond complexes. In addition, the QTAIM (quantum theory of atoms in molecules) [31] has been used to analyze the chemical bond between two adjacent atoms.The QTAIM topological analysis was carried out by the AIMAll program [32]. Furthermore, the SAPT method [33, 34] has been utilized to decompose the interaction energy of σ-type□π-type and parallel halogen bond by the SAPT2016 [35].

3. Results And Discussion

3.1 Interaction Energies of the σ-type,π-type and parallel halogen bond complexes

Figure 2 illustrates the geometry optimizations structures for the minimum energy of σ-type,π-type and parallel halogen bond complexes of the pyrazine and XF (X=F,Cl,Br and I) .For all types of halogen atom X=F, Cl, Br and I, σ-type and π-type halogen-bonded minimum was located. However parallel halogen-bonded minima were only found for X = Cl, Br or I. The interaction energies of these parallel halogen bond□σ-type and π-type halogen bond complexes are shown in Table 1.

Table 1

ΔE, BSSE and with BSSE correction (ΔE^{CP}) in kcal/mol.$V_{s.max}$ in kcal/mol related with the X of XF and $V_{s,min}$ on the XF surface

σ-type halogen bond complexes	MP2/aug-cc-pVTZ			CCSD(T)/aug-cc-pVTZ			
	ΔE	BSSE	ΔE^{cp}	ΔE	BSSE	ΔE^{cp}	$V_{s,max}$
$C_4H_4N_2$-F_2(I)	-2.31	0.63	-1.68	-2.22	0.51	-1.71	8.4
$C_4H_4N_2$-ClF (I)	-14.14	1.52	-12.62	-13.78	1.21	-12.57	39.4
$C_4H_4N_2$-BrF(I)	-22.68	5.16	-17.53	-21.57	4.73	-16.84	40.8
$C_4H_4N_2$-IF(I)	-24.24	4.99	-19.25	-23.68	4.21	-19.47	46.4
π-type halogen bond complexes	ΔE	BSSE	ΔE^{cp}	ΔE	BSSE	ΔE^{cp}	$V_{s,min}$
$C_4H_4N_2$-F_2 (II)	-1.90	0.74	-1.16	-1.73	0.62	-1.11	-2.1
$C_4H_4N_2$-ClF(II)	-4.22	0.97	-3.25	-3.94	0.76	-3.18	-8.6
$C_4H_4N_2$-BrF(II)	-8.32	3.86	-4.46	-7.86	3.51	-4.35	-17.7
$C_4H_4N_2$-IF(II)	-9.34	4.17	-5.17	-8.94	3.56	-5.38	-22.3
Parallel halogen Bondcomplexes	ΔE	BSSE	ΔE^{cp}	ΔE	BSSE	ΔE^{cp}	$V_{s,min}$
$C_4H_4N_2$-ClF(Ш)	-3.21	0.94	-2.27	-2.94	0.78	-2.16	-8.6
$C_4H_4N_2$-BrF(Ш)	-5.36	2.78	-2.58	-5.12	2.45	-2.67	-17.7
$C_4H_4N_2$-IF(Ш)	-5.96	2.83	-3.13	-5.68	2.42	-3.26	-22.3

As shown in the Table 1, the difference of interaction energies corrected for BSSE attained by MP2 and CCSD(T) level has been small. That suggests that MP2/aug-cc-pVTZ provided reliable calculation results for the σ-type, π-type and parallel halogen bond of these investigated dimers. The binding energies of these σ-type, π-type and parallel halogen bond all gradually increased orderly from from X=F to X =I of XF. For σ-type halogen bonded dimers, this order is close accociation with the maximum positive electrostatic potentials ($V_{s,max}$) of the σ-hole related with the X of XF, corresponding coefficients is 0.9717. Relative to the corresponding π-type and parallel halogen bond, this order is close accociation the maximum negative electrostiatic potential ($V_{s,min}$) on the XF surface, corresponding coefficients is 0.9776 and 0.9403, as shown in Figure 3.

A diagrams of the ΔE^{CP} energies of these σ-type, π-type and parallel halogen-bonded minimum structure in Figure 4 reveal that the π-type halogen bonding interactions are weaker than the corresponding σ-type

halogen bonding interactions, and parallel halogen-bond interactions are weaker than the corresponding π-type halogen bonding interactions in $C_4H_4N_2$-XF complexes.

3.2 NBO population analysis.

We used Natural bond orbital (NBO) to analysis the studied σ-type, π-type and parallel halogen-bonded complexes. The value of ΔQ (charge transferred from donor to the acceptor) and ΔE^2 (the second-order perturbation energy) is shown in Table 2. For the σ-type halogen-bonded complexes, the charge transfer from the lone electron pair of the N atom of pyrazine was directed mainly at the X-F antibonding orbitals of the XF. For the π-type halogen-bonded complexes, the charge transfer from the bonding orbitals for the C_4-C_5 in the $C_4H_4N_2$ is mainly refers to the C-N antibonding orbitals of the XF. In regard to parallel halogen-bonded complexes, the charge transfer from the lone electron pair of the F and X atom of XF was directed mainly at the C-N antibonding orbitals of in the $C_4H_4N_2$.

Table 2

The NBO analysis of $C_4H_4N_2$-XF complexes (ΔQ in au, ΔE^2 in kcal/mol)

σ-type halogen bond complexes	**Donor NBOs**	**Acceptor NBOs**	ΔE^2	ΔQ	ΔE^{cp}
$C_4H_4N_2$-F_2(I)	LP N	BD* F - F	4.92	0.014	-1.68
$C_4H_4N_2$-ClF (I)	LP N	BD* Cl- F	83.78	0.154	-12.62
$C_4H_4N_2$-BrF(I)	LP N	BD* Br-F	98.30	0.148	-17.53
$C_4H_4N_2$-IF(I)	LP N	BD* I-F	104.89	0.108	-19.25
π-type halogen bond complexes	Donor NBOs	Acceptor NBOs	ΔE^2	ΔQ	ΔE^{cp}
$C_4H_4N_2$-F_2 (II)	BD C4-C5	BD* F- F	2.83	0.004	-1.16
$C_4H_4N_2$-ClF(II)	BDC4-C5	BD*Cl- F	10.02	0.022	-3.25
$C_4H_4N_2$-BrF(II)	BD C4-C5	BD*Br- F	21.35	0.044	-4.46
$C_4H_4N_2$-IF(II)	BD C4-C5	BD* I- F	38.63	0.050	-5.17
parallel halogen bond complexes	Donor NBOs	Acceptor NBOs	ΔE^2	ΔQ	ΔE^{cp}
$C_4H_4N_2$-ClF(Ш)	LP Cl	BD*N3 - C4	0.16	0.004	-2.27
	LP Cl	BD* C5 - N6	0.16		
	LP F	BD*N3 - C4	0.22		
	LP F	BD* C 5 - N6	0.22		
			(sum 0.76)		
$C_4H_4N_2$-BrF(Ш)	LP Br	BD*N3 - C4	0.21	0.003	-2.58
	LP Br	BD* C5 - N6	0.21		
	LP F	BD*N3 - C4	0.28		
	LP F	BD* C 5 - N6	0.28		
			(sum 0.98)		
$C_4H_4N_2$-IF(Ш)	LP I	BD*N3 - C4	0.24	0.002	-3.13
	LP I	BD* C5 - N6	0.24		
	LP F	BD*N3 - C4	0.36		
	LP F	BD* C5 - N6	0.36		
			(sum 1.20)		

From the amount of ΔE^2, ΔQ and the binding energies ΔE^{CP}, we discovered that the ΔE^2 are concerned with the binding energies (ΔE^{CP}) of σ-type, π-type and parallel halogen bond complexes (See Figure 5), corresponding coefficients 0.9562, 0.9144 and 0.9873, respectively.

As can been in the Table 3, ΔQ has no relevance to the ΔE^{CP} for σ-type and parallel halogen bond complexes. And for the π-type halogen bond complexes, ΔQ has relevance to the ΔE^{CP}, corresponding coefficients is 0.9867 (See Figure 6).

Table 3
A (Electron affinity) and I (Ionisation energy) of the different monomers. Global softness (S) values, f_I^+ and f_c^- (local Fukui functions) in au and local softness (s_I+ or s_c^+) values in au eV^{-1} on the X of XF.

Molecule	I(eV)	A(eV)	S(eV)	f_X^+	f_x^-	s_x^+	s_x^-
F_2	0.055	-0.670	1.379	-0.500	-0.500	-0.690	-0.690
ClF	0.025	-0.500	1.905	-0.722	-0.794	-1.375	-1.513
BrF	0.006	-0.457	2.160	-0.752	-0.813	-1.624	-1.756
IF	-0.010	-0.406	2.525	-0.808	-0.890	-2.040	-2.247

3.3 Research on the conceptual DFT

In the current study, using these reactivity indices, we have studied the reactivity properties of the interacting molecules in σ-type,π-type and parallel halogen bond complexes by the conceptual density functional theory (conceptual DFT). The local softness s(r) is an important factor in quantifying soft-soft interactions (or orbital -controlled reactivity) [36]. It is calculated from s(r) = f (r) S, where f(r) is the Fukui function and S is the global softness of the system.The the global softness S can be approximated as 1/(I-A).I is the vertical ionization energies of the system and A is the electron affinity [37].

The pertinent calculated reactivity indices are shown in Table 3 for different lewis bases and acids considered in σ-type,π-type and parallel halogen bond complexes.For the lewis acids XF (X=F,Cl,Br and I) of the σ-type halogen-bonded complexes, it was revealed that the local softness s^+ on the X of XF is linked to the binding energies (ΔE^{CP}),corresponding coefficients is 0.9752. For the lewis bases XF (X=F,Cl,Br and I) of π-type and parallel halogen bond complexes, it was revealed that the local softness s^- on X of XF is linked to the ΔE^{CP}, corresponding coefficients are 0.9875 and 0.9995 (see Figure 7).

3.4 Topological analysis

The topological analysis of the Laplacian function and its electron charge density is a powerful tool for studying the physical nature of halogen bonding [38, 39].Table 4 displays the topological parameters, including electron density (ρ_b) [40] at the σ-type,π-type and parallel halogen bond critical points, its Laplacian($\nabla^2\rho_b$) and the electron energy density (H_b). The types of interaction can be classified

according to the sign of H_b and $\nabla^2\rho_b$. The halogen bond is generated when the X of XF used as a Lewis acid for the formation of σ-type halogen bond complex. H_b is negative and $\nabla^2\rho_b$ is positive, this corresponds to a partial colvalent interaction [41–43].Nevertheless, the π-type and parallel halogen bond arises when the X of XF acts as lewis bases, both H_b and $\nabla^2\rho_b$ are positive, demonstrating a closed-shell molecular interactions [44].

Table 4

Density (ρ_b), Eigenvalues of the hessian Matrix (λ_1, λ_2 and λ_3), laplacian of ($\nabla^2\rho_b$) and ellipticity(ε) at bond critical points between halogen bond acceptors and halogen bond donors, all units are atomic units.

complexes	ρ_b	λ_1	λ_2	λ_3	$\nabla^2\rho_b$	ε	H_b
$C_4H_4N_2$-F_2(I)	0.0226	-0.0253	-0.0243	0.1774	0.1278	0.0412	-0.0017
$C_4H_4N_2$-ClF (I)	0.0758	-0.0784	-0.0751	0.3124	0.1588	0.0439	-0.0214
$C_4H_4N_2$-BrF(I)	0.0816	-0.0685	-0.0652	0.2812	0.1474	0.0506	-0.0228
$C_4H_4N_2$-IF(I)	0.0878	-0.0512	-0.0485	0.2438	0.1440	0.0557	-0.0148
$C_4H_4N_2$-F_2 (II)	0.0117	-0.0106	-0.0040	0.0700	0.0554	1.6500	0.0029
$C_4H_4N_2$-ClF(II)	0.0169	-0.0124	-0.0034	0.0732	0.0573	2.6471	0.0013
$C_4H_4N_2$-BrF(II)	0.0231	-0.0164	-0.0043	0.0848	0.0641	2.8140	0.0001
$C_4H_4N_2$-IF(II)	0.0241	-0.0139	-0.0034	0.0710	0.0538	3.0882	0.0004
$C_4H_4N_2$-ClF(Ш)	0.0075	-0.0052	-0.0010	0.0353	0.0291	4.2001	0.0015
$C_4H_4N_2$-BrF(Ш)	0.0083	-0.0055	-0.0011	0.0352	0.0285	4.0000	0.0013
$C_4H_4N_2$-IF(Ш)	0.0086	-0.0050	-0.0012	0.0317	0.0255	3.1667	0.0011

On the base of QTAIM, ρ_b (the electron density) should be a reflection of the bond strength. Normally, the greater of the value of the electron density,the greater bond strength.In the Table 4, the value of ρ_b of the σ-type halogen bond complex is from 0.0226 to 0.0878.The amount of ρ_b of the π-type halogen-bonded complexes is from 0.0117 to 0.0241.The amount of the parallel halogen bond complexes is from 0.0075 to 0.0086.The intermolecular forces of σ-type halogen bond complexes are noticeably stronger than that of appropriate π-type or parallel halogen bond complexes. The higher electron densities ρ_b and the greater the interaction energy (ΔE^{CP}), the stronger the σ-type, π-type or parallel halogen bond. The ε (ellipticity) can be defined as λ_1/λ_2-1 and measures the extent to which charge is preferentially accumulated [45].

The ellipticity (ε) supplies a measure of the π properties of a bond. The larger the ellipticity ε, the more obvious π character the bond shows. It can be seen that the ε of the π-type and parallel halogen bond

complexes are much larger than those of the σ-type halogen bond.

3.5 Energy partition by SAPT

Energy decomposition gives us to have a very useful understanding the nature of the studied three types halogen bond interactions [46, 47]. The interactive energy of the three types complexes can be divided into four items:exchange energy, induced energy dispersion energy and electrostatic energy. The results are listed in table 5.

Table 5. Energy decomposition ($kcal \cdot mol^{-1}$) for the σ-type, p-type and parallel halogen bond complexes of $C_4H_4N_2$-XF gained from SAPT

σ-type halogen bond complexes	E_{elst}	E_{ind}	E_{disp}	E_{exch}	E_{int}(SAPT2)	ΔE^{CP}	%E_{elst}	%E_{ind}	%E_{disp}
$C_4H_4N_2$-F_2(I)	-6.02	-3.53	-3.41	11.21	-1.75	-1.68	46.5	27.2	26.3
$C_4H_4N_2$-ClF (I)	-45.18	-32.37	-13.31	78.21	-12.65	-12.62	49.7	35.6	14.6
$C_4H_4N_2$-BrF(I)	-54.14	-31.26	-13.31	81.56	-17.14	-17.53	54.8	31.7	13.5
$C_4H_4N_2$-IF(I)	-40.28	-25.66	-13.12	60.55	-18.51	-19.25	50.9	32.5	16.6
p-type halogen bond complexes	E_{elst}	E_{ind}	E_{disp}	E_{exch}	E_{int}(SAPT2)	ΔE^{CP}	E_{elst}%	E_{ind}%	E_{disp}%
$C_4H_4N_2$-F_2 (II)	-1.87	-1.63	-3.33	5.84	-0.98	-1.16	27.4	23.9	48.8
$C_4H_4N_2$-ClF(II)	-4.60	-4.92	-6.40	13.14	-2.78	-3.25	28.9	30.9	40.2
$C_4H_4N_2$-BrF(II)	-9.09	-8.71	-8.02	21.49	-4.34	-4.46	35.2	33.7	31.1
$C_4H_4N_2$-IF(II)	-7.30	-8.45	-8.87	19.76	-4.86	-5.17	29.7	34.3	36.0
parallel halogen bond complexes	E_{elst}	E_{ind}	E_{disp}	E_{exch}	E_{int}(SAPT2)	ΔE^{CP}	E_{elst}%	E_{ind}%	E_{disp}%
$C_4H_4N_2$-ClF(Ш)	-2.51	-0.57	-5.06	6.05	-2.08	-2.27	30.8	7.0	62.2
$C_4H_4N_2$-BrF(Ш)	-3.48	-0.70	-4.89	6.31	-2.76	-2.58	38.4	7.7	53.9
$C_4H_4N_2$-IF(Ш)	-4.07	-0.84	-5.54	7.07	-3.38	-3.13	38.9	8.0	53.0

As described in talbe 5, the electrostatic energy are the major source of the attraction for the σ-type halogen bonding interactions while the parallel halogen-bond interactions are mainly dispersion energy in $C_4H_4N_2$-XF complexes. For the π-type halogen bonding interactions in $C_4H_4N_2$-XF(X=F and Cl) complexes, electrostatic energy are the major source of the attraction, while in $C_4H_4N_2$-XF(X=Br and I) complexes the electrostatic, induction and dispersion term play equally important role in the total attractive interaction.

4. Conclusions

In present work, the three types halogen bond complexes between pyrazine ($C_4H_4N_2$) and XF (X=F,Cl,Br,I) have been investigated at the MP2/aug-cc-pVTZ level. It can been found that the σ-type halogen bonding interactions are stronger than the corresponding π-type halogen bonding interactions, and π-type halogen-bond interactions are stronger than the corresponding parallel halogen bonding interactions in $C_4H_4N_2$-XF complexes. It can be see that the ΔE^2 are concerned with the binding energies (ΔE^{CP}) for all the σ-type, π-type or parallel halogen bond complexes. The σ-type halogen-bonded complexes are stabilized by electrostatics energy, while the parallel halogen bond complexes are stabilized by dispersion energy. For the π-type halogen bonding interactions in $C_4H_4N_2$-XF(X=F and Cl) complexes, electrostatic term are the major source of the attraction, while in $C_4H_4N_2$-XF(X=Br and I) complexes the electrostatic, induction and dispersion term play equally important role in the total attractive interaction.

Moreover, this study also indicates that the local softness s^+ or local softness s^- on the X of XF is related to the binding energies of σ-type, π-type or parallel halogen bond complexes.

Declarations

Acknowledgments

This research was funded by the National Natural Science Foundations of China (21203135). Some of the calculations described in this study are based on Scgrid of Supercomputing Center of Chinese Academy of Sciences.

Author contribution Junyong Wu: investigation and writing–original draft; Hua Yan: formal analysis and data curation; Hao Chen:visualization; Xianyan Jin:methodology and supervision; Aiguo Zhong: writing-review and editing; Zhaoxu Wang: methodology, software, writing–review and editing; Guoliang Dai: Funding acquisition, methodology, writing–review and editing.

Funding This work was supported by the National Natural Science Foundation of China (Contract no. 21203135)

Data availability Yes.

Code availability N/A.

Conflict of interest The authors declare no competing interests.

References

1. Otte F, Kleinheider UJ, Hiller W, Wang R, Englert U, Strohmann C (2021) J Am Chem Soc, 143(11): 4133–4137
2. Wolf ME, Zhang B, Turney J, Schaefer HF (2019) Phys Chem Chem Phys 21: 6160–6170

3. Kellett CW, Kennepohl P, Berlinguette CP (2020) Nat Commun 11: 1–8
4. Hurtley S, Szuromi P (2017) Science 358: 183–185
5. Legon AC (2010) Phys Chem Chem Phys 12:7736–7747
6. Metrangolo PC, Milani R, Pilati T, Priimagi A, Resnati G, Terraneo G (2016) Chem Rev 116(4):2478–2601
7. Zhu HY, Wu JY, Dai GL (2020) J Mol Model 26(12):1–9
8. Hohenstein EG, Duan J, Sherrill CD (2011) J Am Chem Soc 133:13244 –13247.
9. Zhou FX, Liu Y, Wang ZX, Lu T, Yang QY, Zheng BS (2019) Phys Chem Chem Phys 21(28):15310–15318
10. Wheeler SE (2011) J Am Chem Soc 133:10262–10274
11. Xu H, Cheng J, Yang X, Liu Z, Li W, Li QZ (2017) Chem Phys Chem 18: 2442–2450
12. Holthoff JM, Engelage E, Weiss R, Huber SM (2020) Angew Chem Int Ed Engl 26:59(27):11150-11157
13. Kolá M, Hosta J, Hobza P (2015) Phys Chem Chem Phys 17(35):23279
14. Trnka J, Sedlak R, Kolář M, Hobza P (2013) J Phys Chem A 117(20): 4331–4337
15. Grabowski SJ (2012) J Phys Chem A 116(7):1838–1845
16. Forni A, Pieraccini S, Franchini D, Sironi M (2016) J Phys Chem A 120(45): 9071–9080
17. Murray JS, Lane P, Politzer P (2007) Int J Quantum Chem 107:2286–2292
18. Clark T, Hennemann M, Murray JS, Politzer P (2007) J Mol Model 13:291–296
19. Murray JS, Shields ZP, Seybold PG, Politzer P (2015) J Comput Sci 10:209–216
20. Riley KE, Murray JS, P. Politzer P, Concha MC, Hobza P (2009) J Chem Theory Comput 5: 155–163
21. Peterson KA, Figgen D, Goll E, Stoll H, Dolg M (2003) J Chem Phys 119: 11113–11123
22. PetersonKA , Shepler BC, Figgen D, Stoll H (2006) J Phys Chem A 110: 13877-13883.
23. Frisch MJ, Trucks GW, Schlegel HB et al (2004) GAUSSIAN 03,revision B03. Gaussian, Inc, Wallingford
24. Boys SF(1970) Mol Phys 19:553–566
25. Stanton JF (1997) Chem Phy Lett 281: 130–134
26. Reed AE, Curtiss LA, Weinhold FA (1988) Chem Rev 88:899–926
27. Bulat FA, Toro-Labbe A, Brinck T, Murray JS, Politzer P (2010) J Mol Model 16:1679–1691
28. Geerlings P, Deproft F, Langenaeker W (2003) Chem Rev 103:1793-1983
29. Deproft F, Geerlings P (2001) Chem ReV 101:1451-1464
30. Liu SB (2015) J Phys Chem A 119 (12):3107–3111
31. Bader RFW (1990) Atoms in molecules: a quantum theory. Oxford University Press, Oxford
32. Keith TA (2019) AIMAll, version 19.10.12. aim.tkgristmill.com
33. Jeziorski B, Moszynski R, Szalewicz K (1994) Chem Rev 94:1887–1930
34. Hohenstein EG, Sherrill CD (2010) J Chem Phys 133: 014101–0141012

35. Bukowski R, Cencek W, Jankowski P, Jeziorski B, Jeziorska M,Kucharski SA, Misquitta AJ, Moszynski R, Patkowski K, Rybak S, Szalewicz K, Williams HL, Wormer PES (2016) SAPT2016: An ab initio program for many-body symmetry adapted perturbation theory calculations of intermolecular interaction energies. Sequential and parallel versions. University of Delaware, Newark; University of Warsaw, Warsaw
36. Parr RG, Yang W (1984) J Am Chem Soc 106:4049
37. Parr RG, Pearson RG (1983) J Am Chem Soc 105:7512–7516
38. Amezaga NJM, Pamies SC, Peruchena NM, Sosa GL (2010) J Phys Chem A 114:552–562
39. Syzgantseva OA, Tognetti V, Joubert L (2013) J Phys Chem A 117:8969–8980
40. Bader RFW, Essen H (1984) J Chem Phys 80:1943–1960
41. Geerlings P, Proft FD (2008) Phys Chem Chem Phys 10:3028–3042
42. Cremer D, Kraka E (1984) Angew Chem Int Ed 23:627
43. Bone RGA, Bader RFW (1996) J Phys Chem 100:10892–10911
44. Espinosa E, Alkorta I, Elguero J, Molins E (2002) J Chem Phys 117: 5529–5542
45. Jiajun D, Maza JR, Xu Y, Xu T, Momen R, Kirk SR, Jenkins S (2016) J Comput Chem DOI: 10.1002/jcc.24476
46. Matczak P (2017) Mol Phys 115:364–378
47. Stasyuk OA, Sedlak R, Guerra CF, Hobza P 92018) J Chem Theory Comput 14(7):3440–3450

Figures

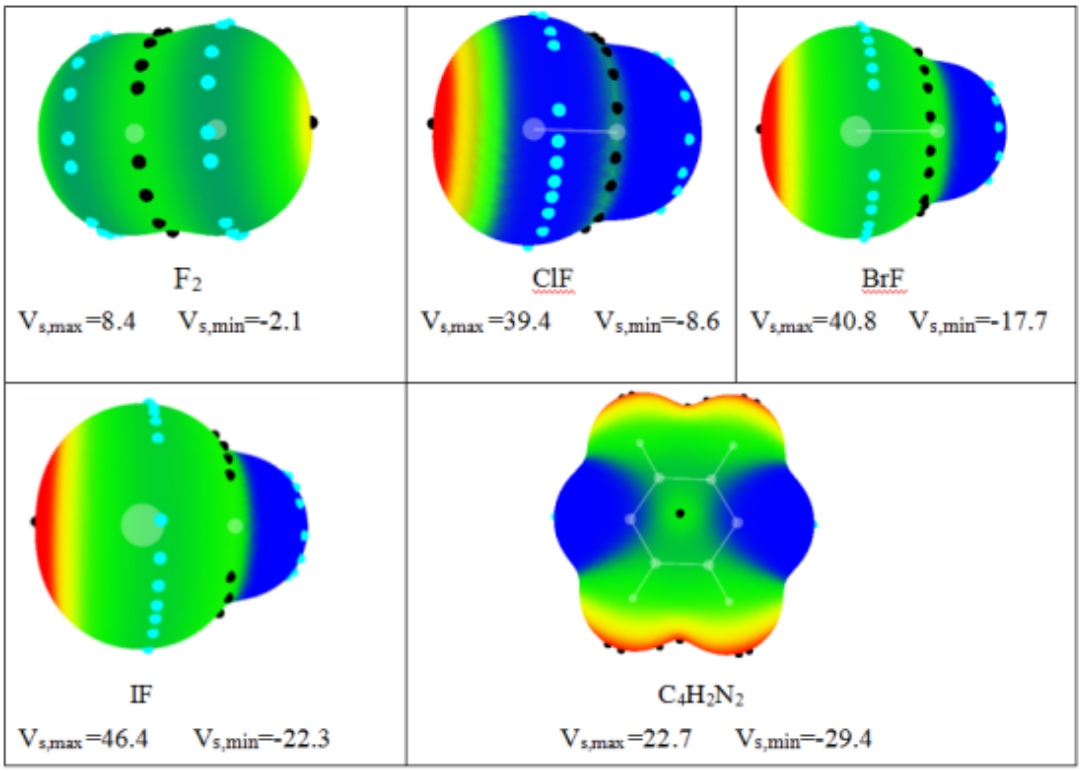

Fig.1 The electrostatic potentials of pyrazine and XF(X=F,Cl,Br and I) on 0.001 au. Color identification: red > 18 kcal/mol, yellow 8-18; green -3-8, blue < -3; Black dots repesent the position of the σ-holes , and the light blue dots are linked with the lone pairs.

Figure 1

See image above for figure legend.

σ - type halogen-bond complexes

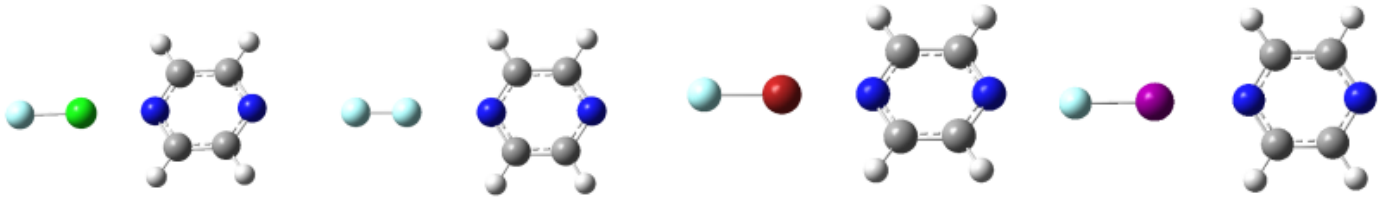

π-type halogen-bond complexes

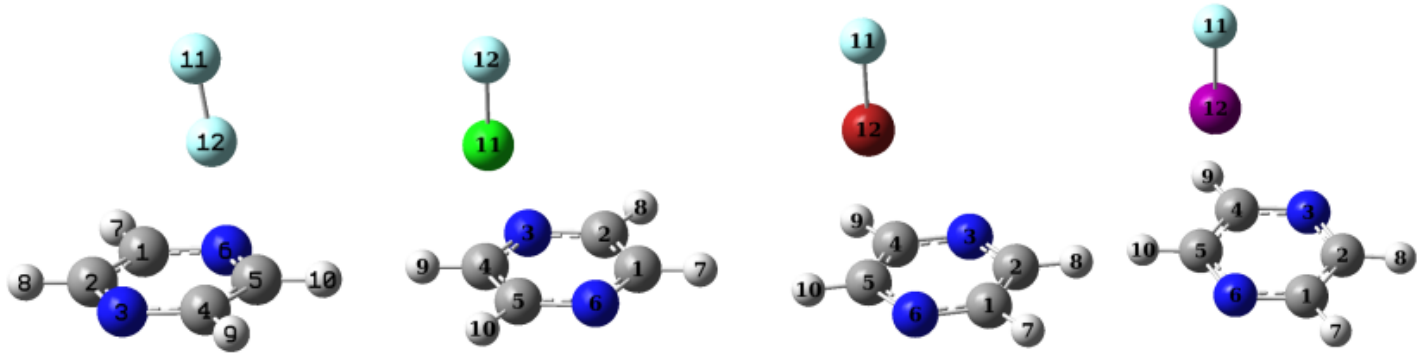

Parallel halogen-bond complexes

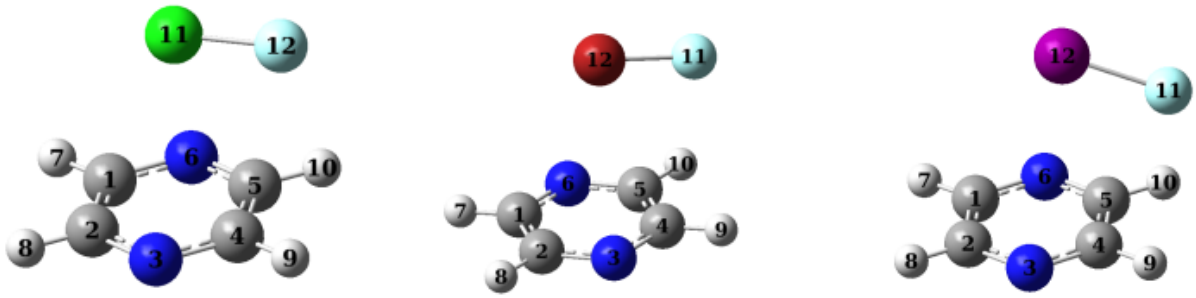

Fig.2 Optimized geometries for the σ-type, π -type, and parallel halogen bond complexes $C_4H_4N_2$-XF (X=F, Cl, Br and I)

Figure 2

See image above for figure legend.

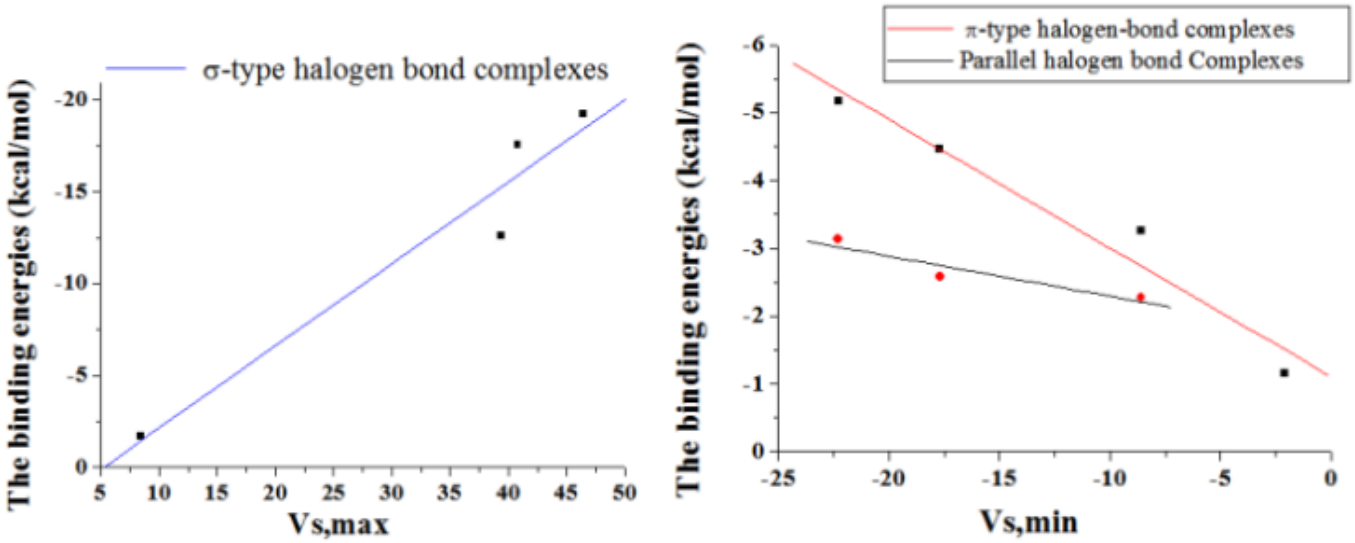

Fig.3 Linear relationships between the binding energies versus the $V_{s,max}$ (most positive electrostatic potentials) related with the X of XF or $V_{s,min}$ (maximum negative electrostatic potential) on the XF surface.

Figure 3

See image above for figure legend.

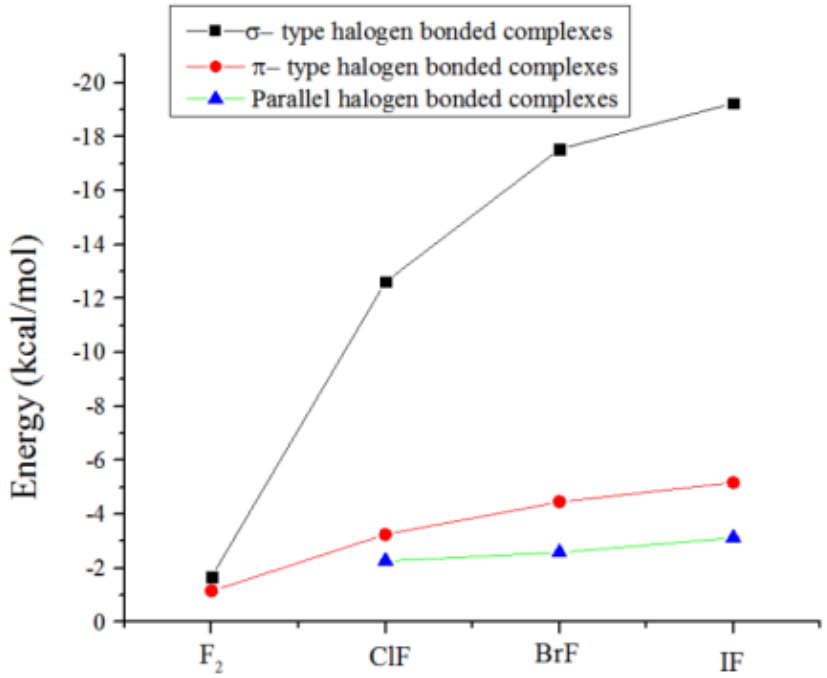

Fig.4 Comparison of the BSSE corrected interaction energies of the three types halogen bond complexes of $C_4H_4N_2$-XF (X=F, Cl, Br and I).

Figure 4

See image above for figure legend.

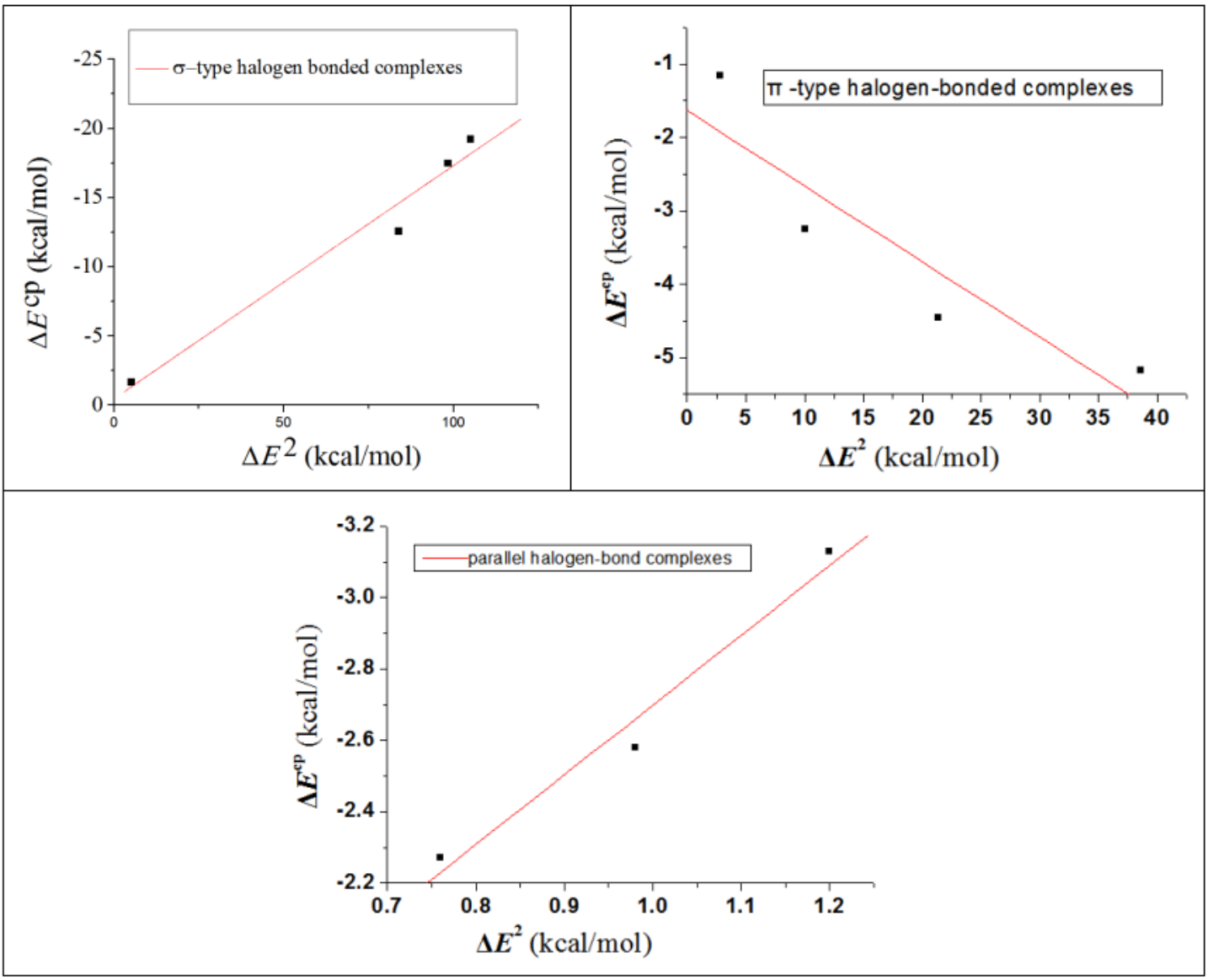

Fig. 5 Correlation between interaction energies and the second-order perturbation energy in the three types halogen bond complexes.

Figure 5

See image above for figure legend.

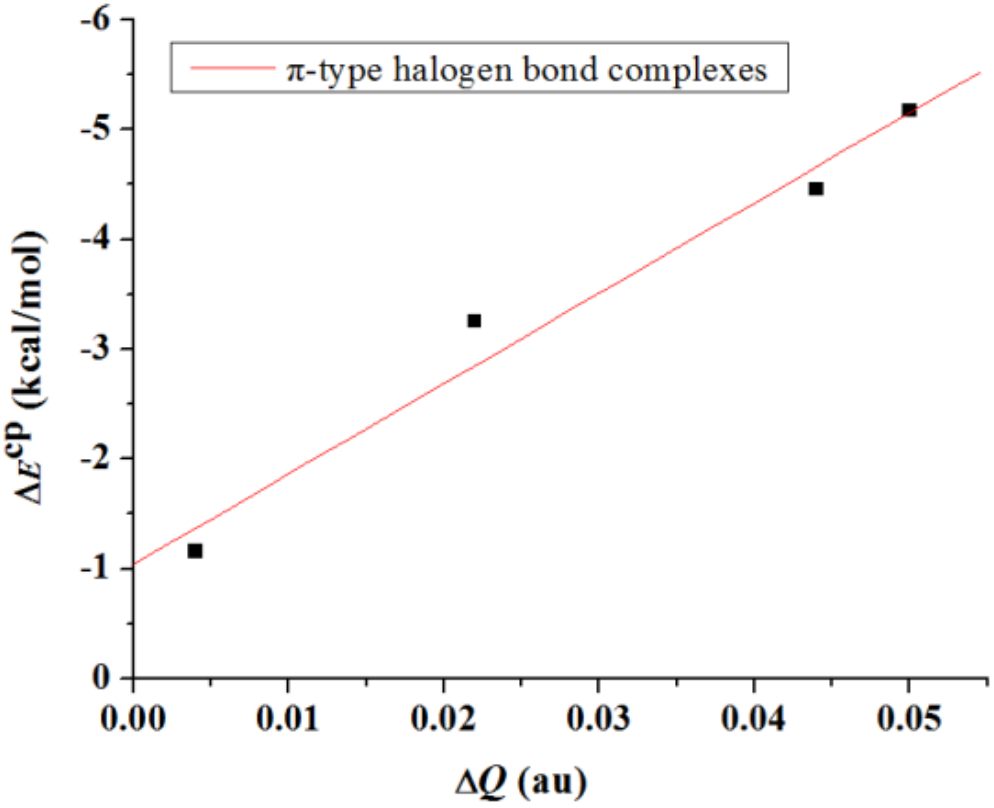

Fig. 6 Correlation between the ΔQ (charge transfer) and the interaction energies in the π -type halogen bond complexes.

Figure 6

See image above for figure legend.

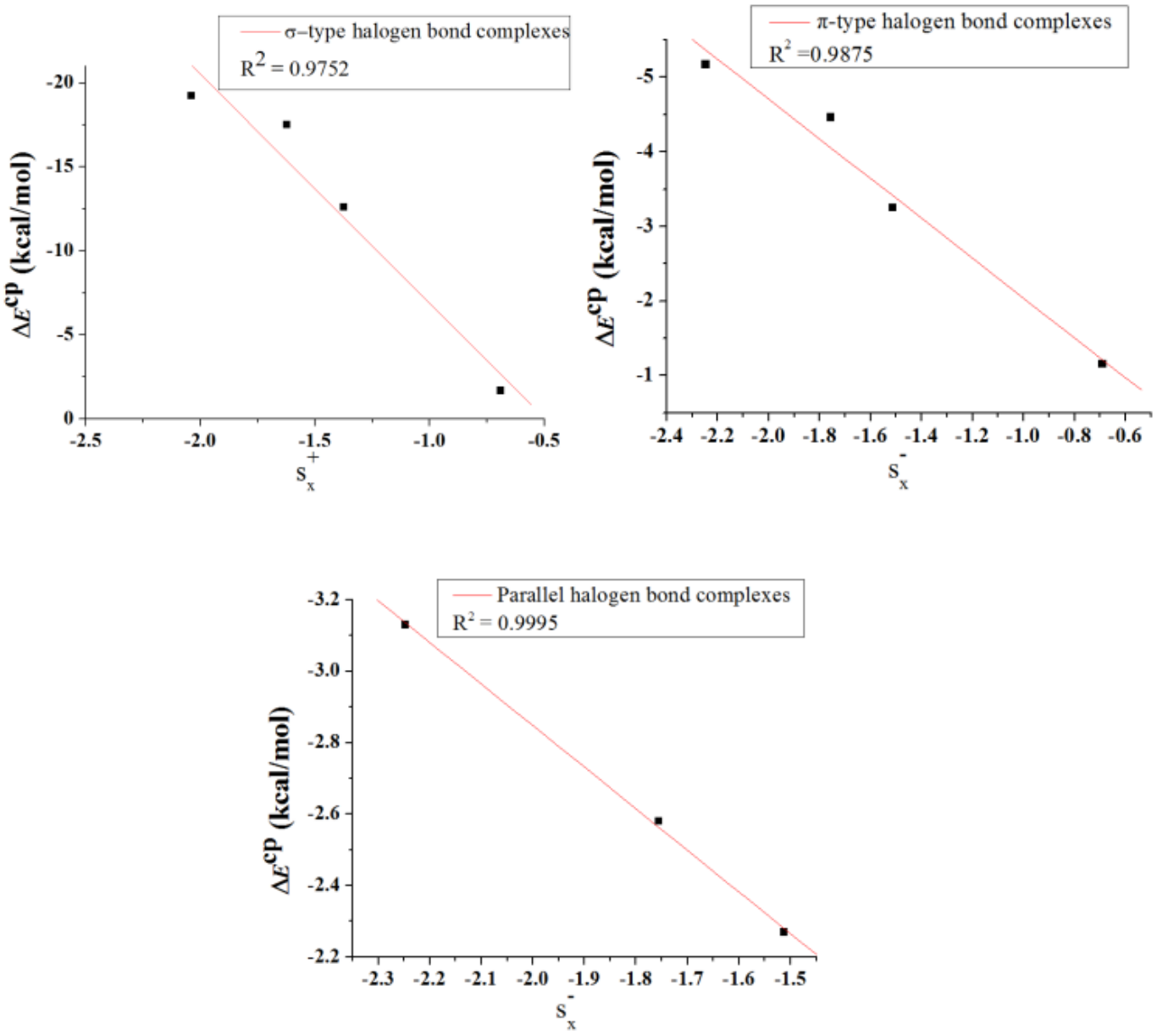

Fig.7 Correlation between the local softness (s_X^+ or s_X^-) values in the XF and the interaction energies of the three types halogen bond complexes.

Figure 7

See image above for figure legend.

Supplementary Files

This is a list of supplementary files associated with this preprint. Click to download.

- Abstractgraphic.doc